European Journal of Phycology
Publication details, including instructions for authors and subscription information:
http://www.tandfonline.com/loi/tejp20

Growth and photophysiological responses of two picoplanktonic Minutocellus species, strains RCC967 and RCC703 (Bacillariophyceae)

Vasco Giovagnetti [a], Maria L. Cataldo [a], Fabio Conversano [a] & Christophe Brunet [a]
[a] Stazione Zoologica Anton Dohrn, Villa Comunale, 80121, Napoli, Italy

Version of record first published: 19 Oct 2012.

To cite this article: Vasco Giovagnetti, Maria L. Cataldo, Fabio Conversano & Christophe Brunet (2012): Growth and photophysiological responses of two picoplanktonic Minutocellus species, strains RCC967 and RCC703 (Bacillariophyceae), European Journal of Phycology, 47:4, 408-420

To link to this article: http://dx.doi.org/10.1080/09670262.2012.733030

Eur. J. Phycol., (2012), **47(4)**: 408–420

Taylor & Francis
Taylor & Francis Group

Growth and photophysiological responses of two picoplanktonic *Minutocellus* species, strains RCC967 and RCC703 (Bacillariophyceae)

VASCO GIOVAGNETTI, MARIA L. CATALDO, FABIO CONVERSANO AND CHRISTOPHE BRUNET

Stazione Zoologica Anton Dohrn, Villa Comunale, 80121, Napoli, Italy

(Received 21 July 2011; revised 25 April 2012; accepted 14 June 2012)

Reaching up to 50% of the total biomass in oligotrophic waters and armed with a set of ecological and biological properties related to their small size, picophytoplankton (<3.0 μm) are a good model to address ecophysiological questions regarding phytoplankton biodiversity. Two picoplanktonic diatoms, one isolated from an upwelling ecosystem in the Pacific Ocean (*Minutocellus* sp., strain RCC967), and another from oceanic waters in the Indian Ocean (*Minutocellus* sp., strain RCC703) were used to test hypotheses on the functional relation between ecological niche adaptation and photosynthetic regulation capacity and efficiency. Cultures were subjected to five sine light climates, each one set to peak at a different photon flux density, respectively 10, 50, 100, 250 and 500 μmol photons $m^{-2}s^{-1}$. Growth rate, photosynthesis, non-photochemical fluorescence quenching, pigment composition, and particulate organic carbon and nitrogen content were followed daily for 5 days. Growth rate and physiological response curves were different in the two species, in agreement with their distinct habitats of origin. Such differences could be related to the diverse photoacclimative strategies displayed by the two species, revealing a clear adaptive divergence despite their close taxonomic relationship. Photoacclimative strategies of the two picoplanktonic diatoms are discussed in the light of functional diversity and ecosystem adaptation.

Key words: diatoms, photoacclimation, photoregulation, picoeukaryotes, non-photochemical fluorescence quenching, xanthophyll cycle

Introduction

Diatoms (Bacillariophyceae) are photosynthetic O_2-evolvers ubiquitous in marine ecosystems. They comprise perhaps 200 000 different species and constitute the most prominent and diversified group of eukaryotic phytoplankton populating the ocean, with a wide range of cell size and shapes (Kooistra *et al.*, 2007; Armbrust, 2009). They are responsible for approximately 40% of oceanic primary production and hence are essential players in the oceanic carbon pump process, as well as in biogeochemical cycling of silicon (because their frustule is composed of silica) and nitrogen (Smetacek, 1999; Armbrust, 2009). Because diatoms are involved in most spring blooms in coastal areas and are characterized by an impressive ecological and biological diversity, the scientific community has dedicated much effort to expanding knowledge of diatom ecophysiology and biology. Indeed, diatom diversity has been examined at the functional level, by studying their adaptations to the abiotic properties of the ecosystems in which they grow (Strzepek & Harrison, 2004; Lavaud *et al.*, 2007; Dimier *et al.*, 2007*b*), and by investigating the genes and functions involved in energy flow from irradiance to biomass (Wilhelm *et al.*, 2006).

Nutrient availability and light, the latter being occasionally limiting or inhibiting, strongly affect phytoplankton growth and thus can be considered as key abiotic factors for algal adaptation to aquatic ecosystems. In the pelagic ecosystem, light is one of the most relevant environmental variables that regulate phytoplankton growth rate, among which it shows the widest fluctuations over a large range of temporal and spatial scales (MacIntyre *et al.*, 2000). Therefore cells need to continuously adjust their photoacclimative state to cope with changes in light intensity, in order to maximize their photosynthetic rate and prevent photoinhibition or photodamage due to harmful excitation-energy pressure (Raven & Geider, 2003). In order to accomplish such cellular tasks, higher plants and algae have evolved several photoprotective mechanisms, among which non-photochemical fluorescence quenching (NPQ) is

Correspondence to: Christophe Brunet. E-mail: christophe.brunet@szn.it

ISSN 0967-0262 print/ISSN 1469-4433 online/12/04000408–420
http://dx.doi.org/10.1080/09670262.2012.733030

the fastest photoprotective reaction, leading to thermal dissipation of excessive irradiance energy in photosystem II (PSII; Li *et al*., 2009; Lepetit *et al*., 2012). NPQ development is mainly controlled by the activation of the xanthophyll cycle (XC; Goss & Jakob, 2010; Lepetit *et al*., 2012). As in most chlorophyll (Chl) *c*-containing phytoplankton species, in diatoms the xanthophyll cycle consists of a single and reversible de-epoxidation step, in which the epoxy carotenoid diadinoxanthin (Dd) is converted to the epoxy-free carotenoid diatoxanthin (Dt), referred to as the diadinoxanthin cycle (Stransky & Hager, 1970; Goss & Jakob, 2010). Diatoms also possess the violaxanthin (Vx) cycle, which contains two de-epoxidation steps in which Vx is converted to zeaxanthin (Zx), through antheraxanthin (Ax) (Lohr & Wilhelm, 1999, 2001). These pigments are mainly involved in the photoprotective biosynthetic pathway of the Dd cycle (Lohr & Wilhelm, 1999, 2001; Dimier *et al*., 2009*a*).

The hypothesis that the capacity for regulating photosynthesis is a functional trait in algae, i.e. an adaptive property of the organism in relation to the ecosystem, has already been discussed and partially demonstrated by different authors (Strzepek & Harrison, 2004; Lavaud *et al*., 2007; Dimier *et al*., 2009*b*). Diatoms have been shown to be highly competitive under fluctuating light climates, because of very efficient processes of photoprotection occurring on time scales of minutes to hours (Wagner *et al*., 2006; Lavaud *et al*., 2007; Brunet & Lavaud, 2010). Indeed, NPQ is greatly enhanced in diatoms (Lavaud *et al*., 2002*a*, 2002*b*, 2004, 2007; Grouneva *et al*., 2009).

As well as in many biological properties and in their different shapes, diatoms are greatly diversified in terms of cell size, ranging from a few micrometres to a few millimetres (Kooistra *et al*., 2007; Armbrust, 2009). Cell size is one of the most relevant functional traits in the ecology of phytoplankton (Litchman & Klausmeier, 2008; Finkel *et al*., 2010). Picophytoplankton (<3 µm, Vaulot *et al*., 2004) are important contributors to marine primary production and can dominate oligotrophic water ecosystems (up to 50% of the total biomass and organic carbon production; Not *et al*., 2005; Worden & Not, 2008). The tiny cell size confers important ecological and biological properties on picophytoplankton, such as a low sinking rate, a low package effect and efficient light utilization (Raven, 1998; Raven *et al*., 2005). Studies on the diversity and ecology of small organisms (Le Gall *et al*., 2008; Vaulot *et al*., 2008; Key *et al*., 2009; Finkel *et al*., 2010), as well as on picoeukaryote ecophysiology (Dimier *et al*., 2007*a*, 2009*a*, 2009*b*; Six *et al*., 2008, 2009; Giovagnetti *et al*., 2010), are gaining momentum. However, to our knowledge, works conducted on picoeukaryotic diatoms are still lacking.

The photophysiological properties of two small-sized diatoms (belonging to the same genus, *Minutocellus*, but with distinct ecological niches) have been investigated, comparing the relation between irradiance, growth capacity and photosynthetic regulation in the two species. The general purpose of this work is to better understand how the photophysiological functional diversity relates to niche adaptation. Physiological response curves (PRC) of the two diatoms were studied by subjecting cultures to five sine light climates, each one set to peak at maximal photon flux densities (PFDs) of 10, 50, 100, 250, 500 µmol photons $m^{-2} s^{-1}$, for 5 days (Giovagnetti *et al*., 2010). Growth and photosynthetic rates, together with particulate organic carbon (POC) and nitrogen (PON) concentrations, as well as pigment changes and non-photochemical fluorescence quenching, were measured daily.

Materials and methods

Algal model and culture conditions

Minutocellus sp. strain RCC967 (Bacillariophyceae) was isolated at a depth of 40 m from the upwelling waters of the Chile coast (Pacific Ocean), while *Minutocellus* sp. strain RCC703 was isolated at a depth of 100 m near the coast in the Indian Ocean (Le Gall *et al*., 2008). Both species were provided by the Roscoff Culture Collection (Vaulot *et al*., 2004). Genome sequencing of the species *Minutocellus* RCC703 is currently ongoing at the Genoscope (Centre National de Séquençage, France; see www.sb-roscoff.fr/Phyto/RCC/).

The strains were grown non-axenically at 20°C at 100 µmol photons $m^{-2} s^{-1}$ with a 11:13 h light:dark photoperiod, in f/2 medium (Guillard & Ryther, 1962) made with locally obtained and sterilized seawater, using 225 cm^2 polystyrene canted neck flasks (Corning, NY, USA). Cells were gently aerated and maintained in exponential phase by daily and semi-continuous dilution (to 50% of the total volume), over a period of more than 2 weeks before the experiment started. Before performing the experiment, the pre-acclimation of the two diatoms to the light climate was checked by assessing the stability of pigment content and growth rate.

Experimental design and sampling strategy

Experimental conditions and sampling strategy were as described in Giovagnetti *et al*. (2010). Once acclimation and stability were achieved, cultures were transferred to five sine light regimes set to peak at PFDs of 10 (LL1 = low light 1), 50 (LL2 = low light 2), 100 (ML = moderate light), 250 (HL1 = high light 1) and 500 (HL2 = high light 2) µmol photons $m^{-2} s^{-1}$ (Fig. 1). These conditions corresponded to a daily-integrated PFD of 0.17, 0.86, 1.71, 4.28 and 8.55 mol photons $m^{-2} d^{-1}$, respectively.

Experiments were conducted using three flasks per treatment during 5 days, and three samples were taken per day. The first sampling was carried out at dawn (the HL2 incident PFD was lower than 40 µmol photons $m^{-2}s^{-1}$), the second at the PFD peak, while the third was taken at sunset (the HL2 incident PFD was lower than 40 µmol photons $m^{-2}s^{-1}$).

Light was provided by the Advanced Control Lighting System (ACLS) and Infinity XR4 (Aquarium Technologies, Sfiligoi S.r.l., Bassano del Grappa, Italy). XR4 was equipped with a HQI metal halide lamp (10000 K). The irradiance was measured using a laboratory PAR 4π sensor (QSL 2101, Biospherical Instruments, San Diego, CA, USA). Temperature and pH were checked daily using an HI-9214-Stick pH meter (Hanna Instruments, Woonsocket, RI, USA).

Twenty to fifty millilitres of culture were collected during each sampling time to carry out measurements of quantum yield of fluorescence, non-photochemical fluorescence quenching, P–I curves, pigments, absorption spectra, cell concentration (by microscopic counts), and size and volume (by Coulter Counter analysis), and particulate organic carbon and nitrogen concentration.

Growth rate was estimated from cell concentration measurements using the following equation:

$$\mu = \ln\left[N_{t_2}/N_{t_1}\right]/[t_2 - t_1] \quad (1)$$

where μ is the growth rate (day^{-1}) and N_t is the mean cell concentration at time t, and t_1 and t_2 correspond to the morning sampling times of days 1 and 2, respectively. From the growth rate, the number of cell divisions (n) per day was estimated using the following equation:

$$n = \mu/[\ln(2)] \quad (2)$$

where n is the number of cell divisions per day and μ is the growth rate.

Pigment analysis

A 10-ml aliquot of algal culture was filtered onto GF/F glass-fibre filters (Whatman, Maidstone, UK) and

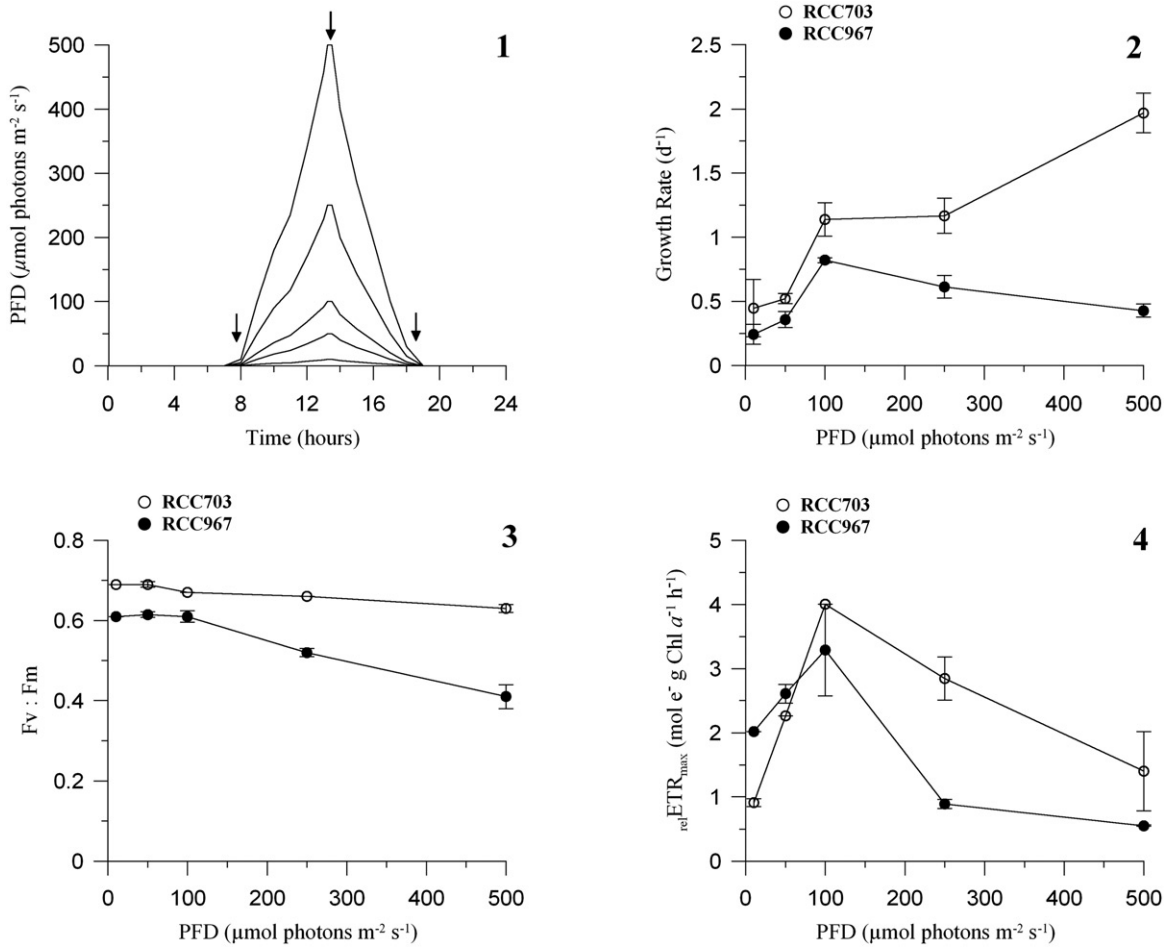

Fig. 1. Scheme of the five sine light conditions, peaking at maximal PFD of 10, 50, 100, 250 and 500 µmol photons $m^{-2}s^{-1}$ (arrows indicate sampling times). **Figs 2–8.** Evolution of the growth rate (d^{-1}; Fig. 2), photosystem (PS) II maximal photochemical efficiency (Fv:Fm; Fig. 3), maximal relative electron transport rate ($_{rel}ETR_{max}$, in mol e^- g Chl $a^{-1}h^{-1}$; Fig. 4), quantum yield of electron transport (α^B, in mol e^- g Chl $a^{-1}h^{-1}$ [µmol photons $m^{-2}s^{-1}]^{-1}$; Fig. 5), light saturation index (Ek, in µmol photons $m^{-2}s^{-1}$; Fig. 6), Chl *a*-specific absorption coefficient (a^*_{ph}, in m^2 mg Chl a^{-1}; Fig. 7), and chlorophyll *a* cellular content (10^{-16} mol Chl *a* $cell^{-1}$; Fig. 8), over the light conditions, in the two species. *Minutocellus* sp. RCC703: open circles; *Minutocellus* sp. RCC967: filled circles. Data are means with $n = 3$; error bars are ±SD.

immediately stored in liquid nitrogen until further analysis. Triplicate samples were taken during each sampling time. Analysis was carried out following the procedure described in Dimier *et al.* (2007*a*). The pigment extract was injected in a Hewlett Packard series 1100 HPLC (Hewlett-Packard, Kennett Square, PA, USA) using a C_8 BDS 3 µm Hypersil, IP column (Thermo Fisher Scientific, Waltham, MA, USA). The mobile phase was composed of eluent A, a solvent mixture of methanol and aqueous ammonium acetate (70:30, v:v), while eluent B was methanol. Pigments were detected spectrophotometrically at 440 nm using a Model DAD, Series 1100 Hewlett-Packard photodiode array detector. Fluorescent pigments were detected in a Hewlett-Packard standard FLD cell series 1100, with excitation and emission wavelengths set at 407 and 665 nm, respectively. For determination and quantification of pigments, calibration curves were obtained using pigment standards from Danish Hydraulic Institute (DHI) Water & Environment (Hørsholm, Denmark).

PAM fluorometer measurements

At the PFD peak, samples were collected for pulse amplitude fluorescence (PAM) measurements. Photochemical efficiency of photosystem (PS) II was estimated by a Phyto-PAM fluorometer (Heinz Walz, Effeltrich, Germany). Triplicate variable fluorescence analysis was performed on 15-min dark-acclimated samples, to measure the maximal photochemical efficiency (Fv/Fm, dark-acclimated samples). Fm was measured after a saturating pulse of red light (2400 µmol photons $m^{-2}s^{-1}$, lasting 450 ms), causing a complete reduction of the PSII acceptor pool.

The non-photochemical quenching of fluorescence (NPQ) was quantified by the Stern–Volmer expression:

$$\mathrm{NPQ} = (\mathrm{Fm}/\mathrm{Fm}') - 1 \qquad (3)$$

Electron transport rate (ETR) vs irradiance (I) curves were determined applying 10 increasing photon flux densities (PFDs; from 1 to 1500 µmol photons $m^{-2}s^{-1}$ for 2 min each).

The relative electron transport rate, normalized by Chl *a* concentration ($_{\mathrm{rel}}\mathrm{ETR}_{\max}$ expressed in mol e^- g Chl $a^{-1}h^{-1}$) was calculated as follows:

$$_{\mathrm{rel}}\mathrm{ETR}_{\max} = (\mathrm{Fv}'/\mathrm{Fm}') \cdot \mathrm{I} \cdot \left(a^*_{\mathrm{ph}}/2\right) \qquad (4)$$

where I is the incident PFDs (expressed in µmol photons $m^{-2}s^{-1}$). The mean Chl *a*-specific absorption coefficient a^*_{ph} of phytoplankton was obtained by Chl *a* normalization (m^2 mg Chl a^{-1}) and divided by 2, assuming that half of the absorbed light was distributed to PSII.

The ETR–irradiance curves were fitted with the equation of Eilers & Peeters (1988) to estimate the photosynthetic parameters α^B, Ek and $_{\mathrm{rel}}\mathrm{ETR}_{\max}$.

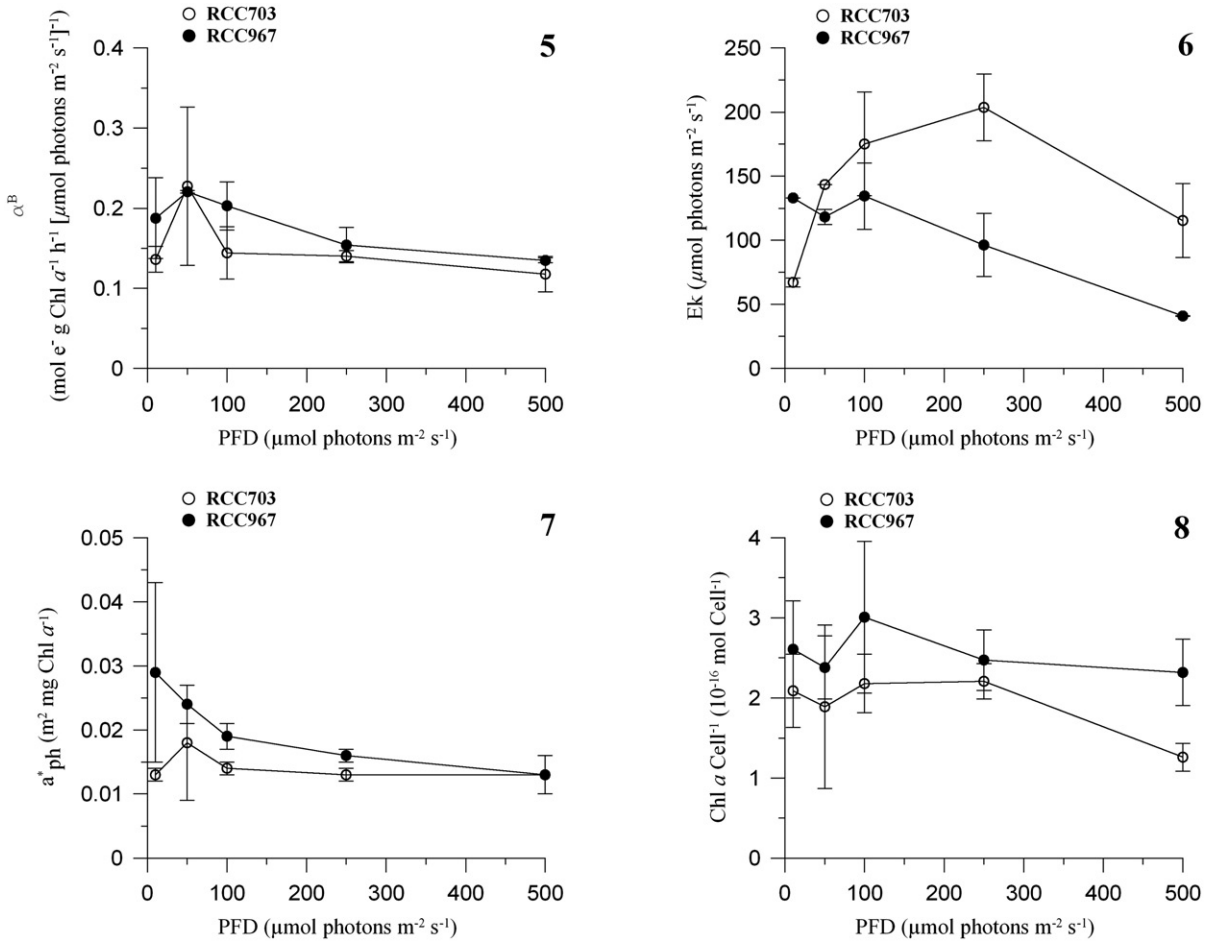

Fig. 1. Continued.

Absorption spectrum

A 10-ml aliquot of algal culture was filtered onto Whatman GF/F filters and immediately frozen. Measurements were carried out following the procedure described in Giovagnetti *et al.* (2010). Absorption was measured between 280 and 800 nm with 1-nm increments on a spectrophotometer (Hewlett-Packard HP-8453E) equipped with an integrating sphere RSA-HP-53 (Labsphere, North Sutton, NH, USA). The mean absorption value (a^*) was thus normalized by the Chl *a* concentration of the sample to obtain the Chl *a*-specific absorption coefficient (a^*_{ph}; m^2 mg Chl a^{-1}).

Particulate organic carbon and nitrogen content

Samples for the determination of particulate organic carbon (POC) and nitrogen (PON) were filtered on pre-combusted (450°C, 5 h) glass-fibre filters (Whatman GF/F) and immediately stored at −20°C. The analyses were performed with a Thermo Scientific FlashEA 1112 automatic elemental analyser (Thermo Fisher Scientific, Waltham, MA, USA), following the procedure described by Hedges & Stern (1984). Cyclohexanone-2,4-dinitrophenylhydrazone was used as standard.

Results

Growth and cell parameters

A wide range of light was suitable for growth of both *Minutocellus* RCC967 and RCC703. A maximal mean cell concentration of $2.26 \pm 0.21 \times 10^5$ cells ml^{-1} was reached by *Minutocellus* RCC967, while for *Minutocellus* RCC703 the maximal mean cell density was $4.35 \pm 0.12 \times 10^5$ cells ml^{-1}.

In *Minutocellus* RCC967 cultures, the maximal chlorophyll (Chl) *a* mean concentrations were 0.11 ± 0.04, 0.15 ± 0.01, 0.26 ± 0.08, 0.50 ± 0.05 and 0.24 ± 0.05 µg Chl *a* ml^{-1} under LL1, LL2, ML, HL1 and HL2, respectively, while in *Minutocellus* RCC703 cultures, they were 0.07 ± 0.02, 0.10 ± 0.05, 0.35 ± 0.05, 0.39 ± 0.02 and 0.48 ± 0.03 µg Chl *a* ml^{-1}.

Minutocellus RCC967 grew optimally under moderate light conditions (ML), where it reached its highest growth rate (0.82 ± 0.02; Fig. 2); the growth rate then decreased under high light. In contrast, the growth rate of *Minutocellus* RCC703 gradually increased over the light range, reaching its highest growth rate (1.97 ± 0.15; Fig. 2) at 500 µmol photons $m^{-2}s^{-1}$. The growth rate was higher in *Minutocellus* RCC703 than in *Minutocellus* RCC967 (Fig. 2). The number of divisions per day ranged between 0.35 and 1.18 divisions d^{-1} in *Minutocellus* RCC967 and between 0.65 and 2.84 divisions d^{-1} in *Minutocellus* RCC703.

Very low variability of cell size and volume was found, without any trend related to the growth rate or light conditions. Cell size (considered as the maximum cell dimension obtained by Coulter Counter measurements) ranged between 2.72 ± 0.06 µm and 3.12 ± 0.24 µm in *Minutocellus* RCC967, and between 2.66 ± 0.06 µm and 3.11 ± 0.27 µm in *Minutocellus* RCC703 cultures. Cell volumes ranged between 11.20 ± 0.24 $µm^3$ and 16.19 ± 3.79 $µm^3$ (*Minutocellus* RCC967), and between 9.96 ± 0.70 $µm^3$ and 16.09 ± 4.36 $µm^3$ (*Minutocellus* RCC703).

Photosynthetic parameters and absorption capacity

The maximal quantum yield of fluorescence (Fv/Fm) was stable under LL and ML conditions in both species (Fig. 3). The decrease under HL was stronger in *Minutocellus* RCC967 than in *Minutocellus* RCC703.

The relative electron transport rate ($_{rel}ETR_{max}$) of both species was lower in LL than in ML, in which the photosynthetic rate was maximal (Fig. 4). Under the lowest irradiance (LL1), the photosynthetic rate mean value in *Minutocellus* RCC967 was two-fold higher than in *Minutocellus* RCC703, although the latter performed better under ML and HL conditions. From ML to HL regimes, the decrease of $_{rel}ETR_{max}$ was much greater in *Minutocellus* RCC967 than in *Minutocellus* RCC703 (Fig. 4).

The quantum yield of electron transport (α^B) of *Minutocellus* RCC703 was constant over the light gradient (Fig. 5, ~0.14 mol e^- g Chl $a^{-1}h^{-1}$ [µmol photons $m^{-2}s^{-1}$] $^{-1}$) except under LL2 regime, where it was higher (0.23 ± 0.091 mol e^- g Chl $a^{-1}h^{-1}$ [µmol photons $m^{-2}s^{-1}$]$^{-1}$). In *Minutocellus* RCC967, α^B was higher under the lowest light (Fig. 5, ~0.20 mol e^- g Chl $a^{-1}h^{-1}$ [µmol photons $m^{-2}s^{-1}$]$^{-1}$) while it decreased gradually from moderate to high light.

The light saturation index of photosynthesis (Ek) showed a quite opposite trend between the two species (Fig. 6), again revealing different physiological responses to light. The *Minutocellus* RCC967 Ek was stable (at ~130 µmol photons $m^{-2}s^{-1}$) under LL and ML regimes, gradually decreasing with increasing light. In *Minutocellus* RCC703, Ek increased from 67.10 ± 3.37 (LL1) to 203.64 ± 26.01 µmol photons $m^{-2}s^{-1}$ (HL1), only decreasing again under the highest light (115.47 ± 28.74 µmol photons $m^{-2}s^{-1}$).

In *Minutocellus* RCC967, the Chl *a*-specific absorption coefficient (a^*_{ph}) decreased over the light gradient, whereas it was stable in *Minutocellus* RCC703, with the exception of a slight increase in the LL2 treatment (Fig. 7). In both species, similar a^*_{ph} values were found under HL conditions. These results underline that a different acclimation strategy was

adopted by the two species in the regulation of the light absorption capacity, under low or moderate light.

The Chl *a* content per cell differed between the two diatoms only in the HL2 treatment (Fig. 8). Values ranged between $2.32 \pm 0.42 \times 10^{-16}$ and $3.01 \pm 0.95 \times 10^{-16}$ mol Chl *a* cell^{-1} in *Minutocellus* RCC967 and between $1.26 \pm 0.17 \times 10^{-16}$ and $2.21 \pm 0.61 \times 10^{-16}$ mol Chl *a* cell^{-1} in *Minutocellus* RCC703. In both species, the low variations in Chl *a* cellular content were independent from cell size or volume changes, since no significant correlation between Chl *a* cell^{-1} content and cell size was found. In *Minutocellus* RCC967, the Chl *a* cell^{-1} content was stable over the whole experimental light gradient, while in *Minutocellus* RCC703, Chl *a* cell^{-1} almost halved under HL2 (Fig. 8).

Accessory pigments

In *Minutocellus* RCC703, the amounts per cell of the main accessory photosynthetic pigments, Chl c_1 and c_2 and fucoxanthin (Fuco), were significantly correlated with the Chl *a* content per cell (data not shown). This led to a quite stable ratio between accessory pigments and Chl *a*, mainly evident under moderate and high light (Figs 9, 11). In *Minutocellus* RCC967, on the other hand, the main accessory pigments varied independently from the Chl *a* content, so that there was a decrease in the accessory pigments: Chl *a* ratio in ML and HL conditions (Figs 10, 12). These results explain the distribution of absorption capacity of these two diatoms over the light range (Fig. 7).

While in *Minutocellus* RCC967 the *cis*-fucoxanthin (*cis*-Fuco):Chl *a* ratio followed the same trend as Fuco over the light gradient (Fig. 12), in

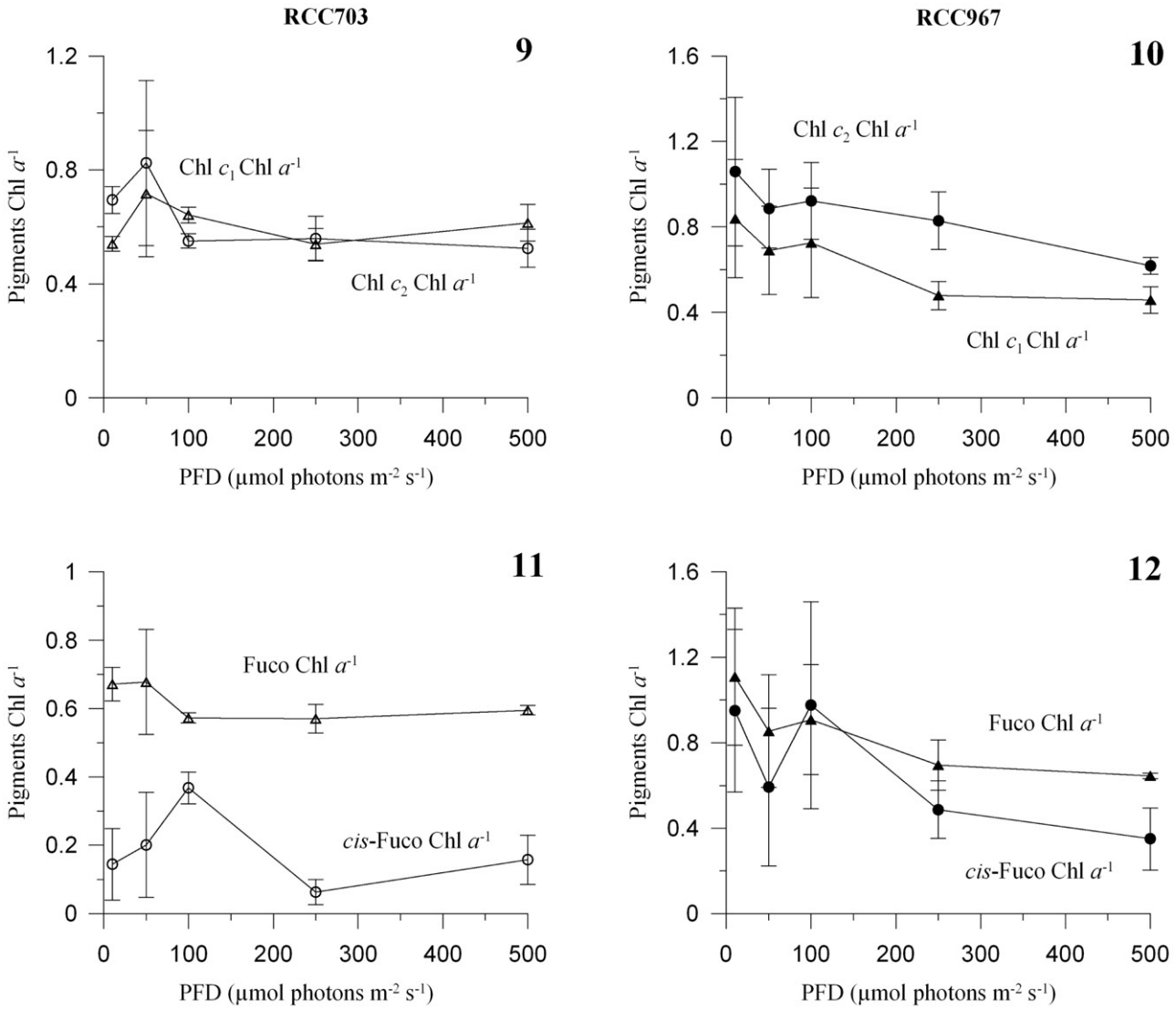

Figs 9–12. Evolution of chlorophyll (Chl) c_1 and c_2 Chl a^{-1} (Figs 9, 10), and fucoxanthin and *cis*-fucoxanthin: Chl *a* (Figs 11, 12), over the light conditions. Chl *a*, chlorophyll *a*; Chl c_1, chlorophyll c_1; Chl c_2, chlorophyll c_2; Fuco, fucoxanthin; *cis*-Fuco, *cis*-fucoxanthin. *Minutocellus* sp. RCC703: open circles and triangles; *Minutocellus* sp. RCC967: filled circles and triangles. Data are means with $n = 3$; error bars are ±SD.

Minutocellus RCC703 it was much more variable, with an opposite trend in LL and ML (i.e. rising towards ML) relative to Fuco (Fig. 11).

In *Minutocellus* RCC703, the β-carotene (β-Car) cell^{-1} content was stable over the light gradient, except for a decrease in the HL2 regime, while in *Minutocellus* RCC967 it was higher and more variable in the LL and ML regimes (data not shown). Interestingly, together with β-Car, we detected low quantities of α-carotene (α-Car) in both diatoms (data not shown), with its cellular content slowly decreasing over the light gradient in both species. Traces of a neoxanthin-like pigment were also found, but given the uncertainty of the pigment determination, we do not discuss this further here; it is an interesting topic for further investigations.

Photoprotection

In both diatoms, the content of Dt + Dd increased from low to high irradiance (Figs 13, 14), being at least two-fold higher in *Minutocellus* RCC967 than in *Minutocellus* RCC703. In *Minutocellus* RCC703, the Dd content per cell reached a plateau under HL conditions, while the Dt cellular content gradually increased over the irradiance gradient (Fig. 15). The de-epoxidation state (DPS) reached a maximal 39% in this diatom (Fig. 17).

In *Minutocellus* RCC967, the xanthophyll cycle was differently regulated. Whereas the Dd cellular content was almost stable over the light gradient (Fig. 16), the Dt cellular content increased steeply (almost 60-fold) from ML to HL conditions (Fig. 16). Consequently, DPS reached 80% (Fig. 18). These results reflect a much more strongly enhanced photoprotective state of *Minutocellus* RCC967 cells compared with those of *Minutocellus* RCC703.

In both diatoms, the development of non-photochemical fluorescence quenching (NPQ) relied strongly on the de-epoxidation of Dd to Dt, as demonstrated by the significant correlation between NPQ and Dt Chl a^{-1} in *Minutocellus* RCC703 ($R^2 = 0.96$, $P < 0.005$) and in *Minutocellus* RCC967 ($R^2 = 0.90$, $P < 0.005$; data not shown). Maximal NPQ mean values of 1.15 ± 0.13 and 0.34 ± 0.02 were reached in *Minutocellus* RCC703 and RCC967, respectively (Figs 19, 20). In both diatoms, NPQ development was significantly correlated with the decrease in the PSII maximal photochemical efficiency with increasing light (Fv:Fm, $P < 0.05$; data not shown).

Another divergence between the two species concerned the two photoprotective xanthophylls of the violaxanthin cycle, antheraxanthin (Ax) and zeaxanthin (Zx), which were present in *Minutocellus* RCC967 but not in *Minutocellus* RCC703. Both pigments increased with increasing light in *Minutocellus* RCC967 and were significantly correlated with Dt cell^{-1} ($P < 0.01$) and NPQ ($P < 0.05$; data not shown).

Organic carbon and nitrogen content

Both the particulate organic carbon (POC) and nitrogen (PON) per cell, and the general trend in these over the light gradient, were quite similar in the two species (data not shown). In both diatoms, POC per cell increased under LL and HL conditions (data not shown). POC and PON per cell were not significantly correlated in *Minutocellus* RCC703 (Fig. 21) but were in *Minutocellus* RCC967 ($P < 0.01$, Fig. 22). Indeed, changes in the POC:PON ratio were stronger and related to the light gradient in *Minutocellus* RCC703 (Fig. 23) than in *Minutocellus* RCC967, in which the ratio was stable (Fig. 24). In *Minutocellus* RCC703, the POC:PON ratio was correlated with the growth rate (Fig. 25), which was not the case in *Minutocellus* RCC967 (Fig. 26).

Discussion

Given the similar cell size of the two *Minutocellus* species and their close taxonomic relationship, the differences in their photophysiological and growth responses to a gradient of light intensities may reflect adaptation to distinct ecological niches.

Minutocellus RCC703 is an oceanic species which was isolated from 100 m depth in the Indian Ocean. Despite coming from such a depth, this diatom appears to be a high light-adapted species (Falkowski & Owens, 1980; Falkowski *et al.*, 1981), as demonstrated by the fact that the highest growth rate was reached at the highest light. Furthermore, this species performs better than RCC967 under each light condition, indicating more efficient light utilization. Since the Indian Ocean sample from which *Minutocellus* RCC703 was isolated came from near the coast of South Africa (at 35°3'S, 23°44'E), in a system characterized by strong coastal winds occasionally accompanied by extreme convective activity, such as tornadoes during winter (Goliger & Retief, 2002), we hypothesize that cells might have been quickly transported downwards prior to sampling and thus reached the depth of 100 m.

In contrast, the growth of *Minutocellus* RCC967 is inhibited at high light, and the two diatoms clearly have different ecophysiological requirements and photoacclimation strategies to cope with high light. In fact, RCC967 is a species isolated from the Chile upwelling system, in which turbid water masses are transported from deeper layers to the surface.

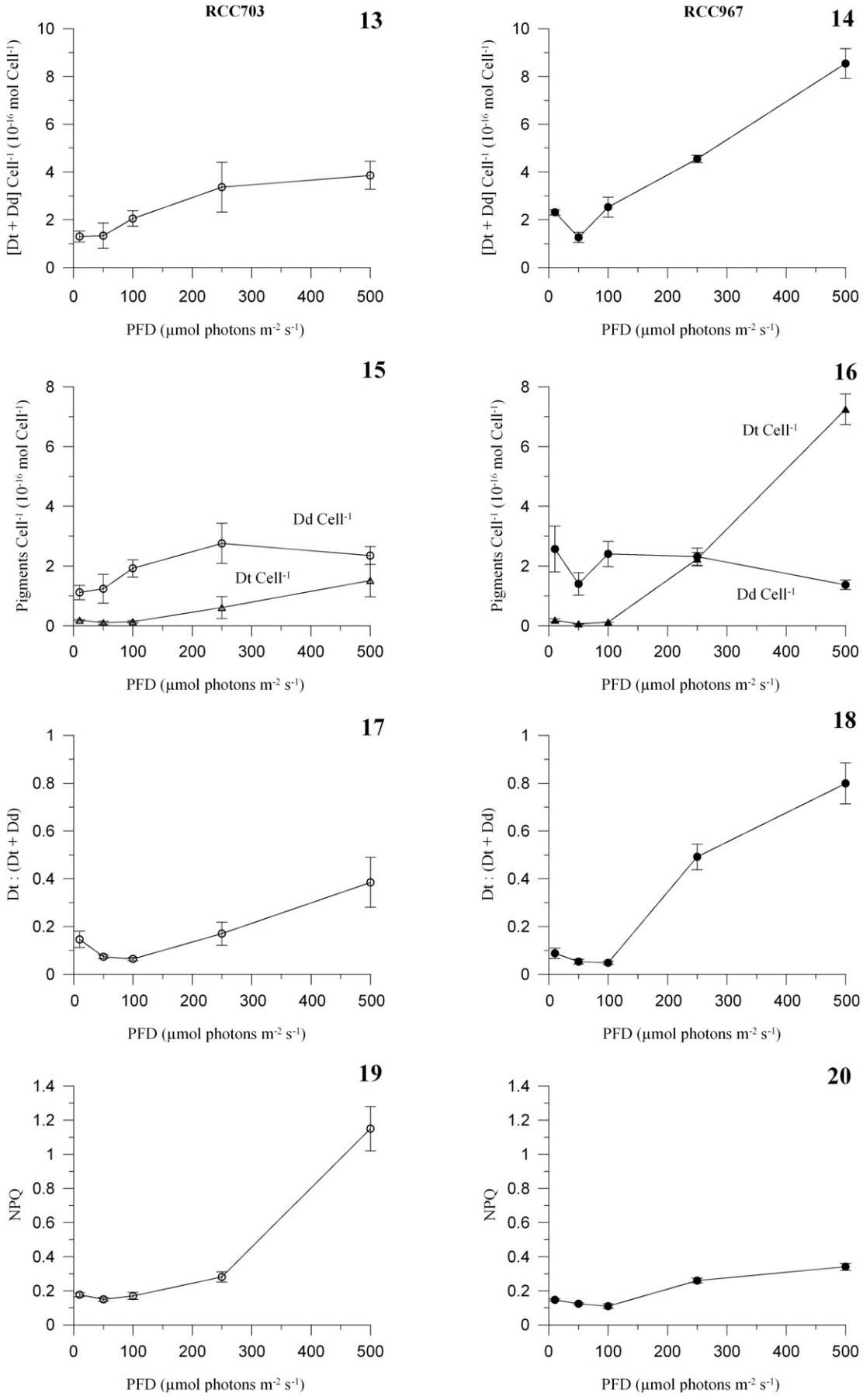

Figs 13–20. Evolution of (Dt + Dd) cell^{-1} (10^{-16} mol pigment cell^{-1}; Figs 13, 14), Dt and Dd cell^{-1} (10^{-16} mol pigment cell^{-1}; Figs 15, 16), [Dt: (Dt + Dd)] DPS (DPS; Figs 17, 18), and NPQ (Figs 19, 20), over the light conditions. Dt, diatoxanthin; Dd, diadinoxanthin; NPQ, non-photochemical fluorescence quenching. *Minutocellus* sp. RCC703: open circles and triangles; *Minutocellus* sp. RCC967: filled circles and triangles. Data are means with $n = 3$; error bars are ±SD.

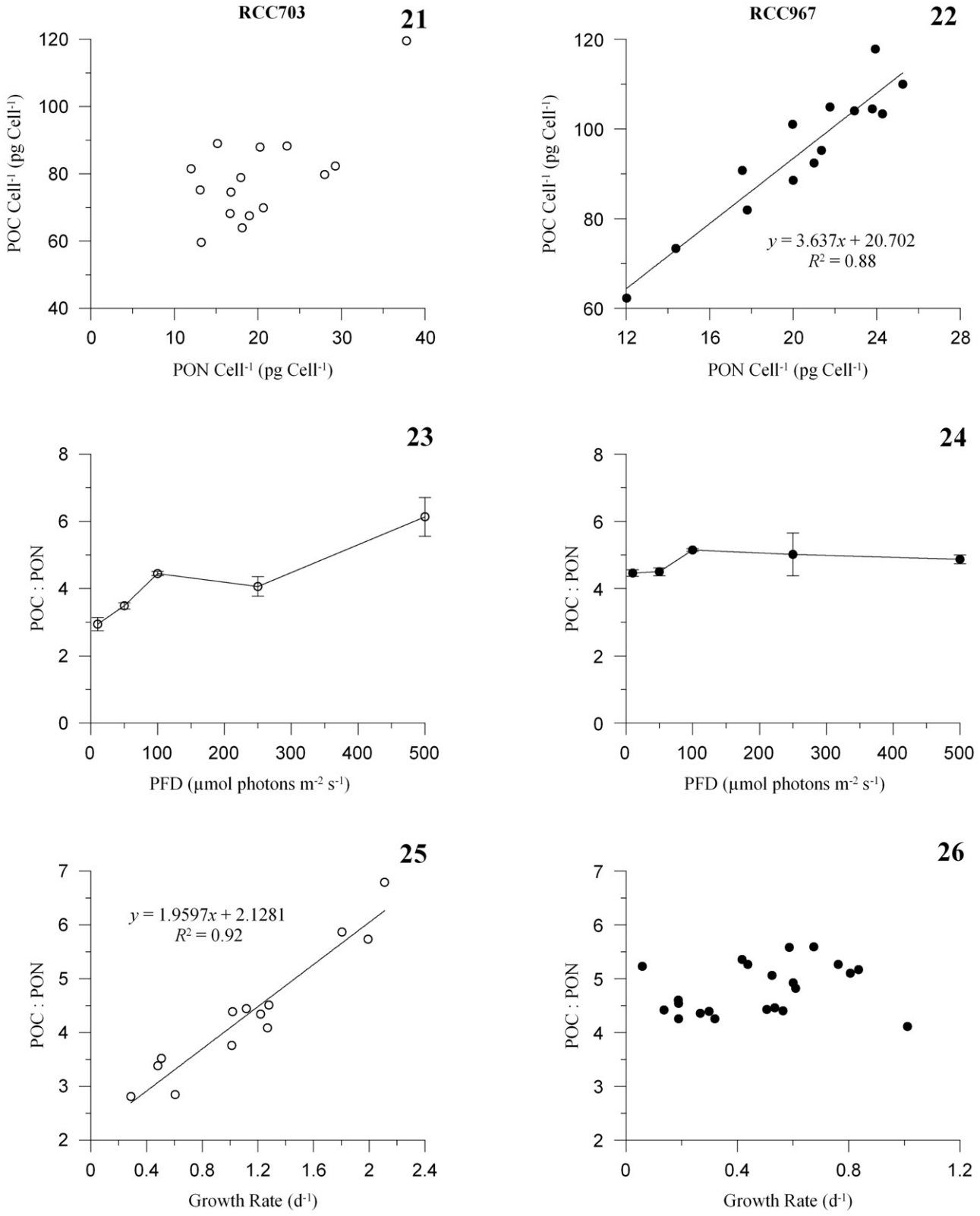

Figs 21, 22. Relationship between particulate organic carbon (POC) and nitrogen (PON, in pg cell^{-1}; Figs 21, 22). **Figs 23, 24.** Evolution of the POC:PON ratio over the light conditions. Data are means with $n = 3$; error bars are ±SD. **Figs 25, 26.** Relationship between growth rate (d^{-1}) and POC:PON ratio. *Minutocellus* sp. RCC703: open circles; *Minutocellus* sp. RCC967: filled circles.

Intriguing is the mismatch between the maximal relative photosynthetic and growth rates in the oceanic species (RCC703), contrary to what occurs in the upwelling species (RCC967), in which the highest $_{rel}ETR_{max}$ and growth rate are both reached at moderate light. This might mean that the growth rate of *Minutocellus* RCC703 is mainly modulated by the maximization of the electron

transport rate within PSII, until the PFD becomes limiting (photosynthetic regulation-dependent growth rate), after which a biochemical regulation channels in parallel the harvested photons into maintaining the growth rate when the PFD becomes saturating or even over-saturating during a portion of the day (biochemical regulation-dependent growth rate). The significant correlation between POC:PON ratio and growth rate highlights how *Minutocellus* RCC703 is able to maintain or increase growth under a wide range of PFDs by tuning intracellular biochemical properties. The strategy adopted by *Minutocellus* RCC967 is different, preventing the biochemical properties of cells from changing over the light gradient, while this species rearranges the PSII antenna organization under high light, as revealed by the changes observed in pigment content and absorption capacity. Compared with *Minutocellus* RCC703, the smaller photophysiological capacity of *Minutocellus* RCC967 to face high light stress might thus be the consequence of its low light acclimation, in agreement with the growth of this diatom in highly turbid waters. We hypothesize that the low light-adapted *Minutocellus* RCC967 is therefore mainly sensitive to the light experienced at the midday peak, determining the regulatory and acclimatory state of the cells and the quantity of energy transferred to photoprotective processes rather than fuelling growth. On the contrary, *Minutocellus* RCC703, which is adapted to high light, is able to cope efficiently with the midday light energy-maximum and acclimates adequately to the daily light dose experienced by cells, hence their enhanced growth.

In *Minutocellus* RCC703, the lack of a significant relationship between the POC and PON per cell, as well as the increase of POC:PON ratio, under high light conditions, might indicate an imbalance in the intracellular molecular pools toward a greater allocation of nitrogen-poor molecules, for instance with a decreasing cellular content of protein (Lynn *et al.*, 2000) or an increase in carbohydrates and lipids (Geider & LaRoche, 2002). The decrease of $_{rel}ETR_{max}$ under HL appears to represent a functional regulation of the photosynthetic rate in response to the HL peak, rather than a net decrease of the species' photosynthetic capacity due to a stressful light. This hypothesis fits the high light-enhanced growth rate and photoacclimation strategy of this diatom. As suggested by our results on accessory pigments and Chl *a* variations, a modification in size or number of PSII, i.e. both light-harvesting antenna complexes and reaction centres, occurs under the highest light tested.

The photoacclimative strategy deployed by *Minutocellus* RCC703 allows this species to keep the quantum yield of electron transport (α^B) and the Chl *a*-specific absorption coefficient (a^*_{ph}) almost constant over the light gradient (with the exception of LL2 condition), ensuring an effective photosynthetic rate under limiting light, which corresponds to the greatest part of the daylight period. Both the photoacclimation strategy and the short-term negative effect of the HL peak on $_{rel}ETR_{max}$ of this species are confirmed by the increase of Ek over the light gradient, excluding the HL2 decrease, which is related to the decrease of photosynthetic pigment content. These results show how this species responds to the high PFD peak with efficient physiological/biochemical variations without compromising growth capacity, confirming the ability to integrate energy-information and adequately respond to both high PFD peak and daily-integrated PFD.

Our results show that *Minutocellus* RCC967 is negatively affected when the light dose is higher than $\sim$2 mol photons $m^{-2} d^{-1}$. This low value confirms this species as low light acclimated, in agreement with its habitat (upwelling water). Moreover, under very low light (e.g. LL1), the photosynthetic rate of *Minutocellus* RCC967 is two-fold greater than that of *Minutocellus* RCC703. This result might be explained by the higher α^B value in *Minutocellus* RCC967 in LL1, as well as the higher a^*_{ph} values in LL1 and LL2, providing a greater photon flux in the PSII antenna, which is also suggested by the higher pigment content in this species relative to *Minutocellus* RCC703.

Minutocellus RCC967 mainly responds to the PFD peak, entering a photoprotective state that lowers the photosynthetic efficiency for light harvesting (i.e. a decrease in α^B), consequently causing a state of light-limitation for cells growth, during the largest portion of the day (when PFD is limiting). *Minutocellus* RCC967 photoprotective strategy probably relies on a σ-type photoacclimation strategy (Six *et al.*, 2008; Dimier *et al.*, 2009*a*; Giovagnetti *et al.*, 2010), regulating the energy flux by decreasing the accessory photosynthetic pigments content in the PSII antenna to achieve a lower light-harvesting capacity. This feature is further enhanced by the huge synthesis of Dt, which greatly persists in cells even under low PFD. In fact, the content of Dd and Dt measured in this species at sunset and dawn is two-fold higher than the content measured in *Minutocellus* RCC703 ($1.5 - 2 \times 10^{-16}$ vs $4 - 5 \times 10^{-16}$ mol (Dt + Dd) $cell^{-1}$, in *Minutocellus* RCC703 and RCC967, respectively), mainly due to the strong increase in Dt ($0.25 - 0.50 \times 10^{-16}$ vs $0.50 - 1.00 \times 10^{-16}$ mol Dt $cell^{-1}$, in *Minutocellus* RCC703 and RCC967, respectively). This photoacclimative strategy is probably possible because of the higher amount of Dd and β-Car molecules in the light-harvesting complex of the PSII of

Minutocellus RCC967, compared with *Minutocellus* RCC703, as well as of the presence of the xanthophylls antheraxanthin (Ax) and zeaxanthin (Zx), with a role of intermediate products during the Dd cycle pigments biosynthetic pathway (Goss & Jakob, 2010). Whereas Dd and Dt increased together with increasing light intensities in *Minutocellus* RCC703, their trends become opposite under HL regimes in *Minutocellus* RCC967, revealing that for a certain PFD and/or Dt content threshold, Dt still increases without any replenishment of Dd. A similar strategy with a very high Dt synthesis has been observed also in the low-light acclimated *Skeletonema marinoi* when subjected to PFD increase (Dimier *et al*., 2007*b*). Such a strong increase, together with the probable low accessibility to the Dt-epoxidase and low level of NPQ, would be related to a photoprotective function of Dt at the level of the thylakoid membrane lipids, against peroxidative stress during excess light energy exposure, as also demonstrated for Zx in higher plants (Havaux & Niyogi, 1999).

The two photoacclimative strategies displayed by the two *Minutocellus* species differ from that deployed by another picoeukaryote, *Phaeomonas* sp. RCC503, subjected to the same experimental conditions (Giovagnetti *et al*., 2010). Under high light, despite the photoprotective state of its cells, *Phaeomonas* RCC503 increases the size of the light-harvesting antenna complexes (by increasing the content of both Chl *a* and accessory photosynthetic pigments) to overcome the loss of photosynthetic efficiency. The striking occurrence of a photoprotective response in synergy with the enhancement of the light-harvesting capacity has been related to the adaptation of this species to the coastal environment (Giovagnetti *et al*., 2010). The reason for this finding might be that cells experience multiple and rapid PFD variations in a basically low-light climate, linked to the water column turbulence, low depth and turbidity of the coastal ecosystem. The comparison of the three picoeukaryotes fits the results obtained by Dimier *et al*. (2009*b*), comparing the ecophysiological properties of six phytoplanktonic species, in which three photophysiological groups (high light-, low light-, and variable light-adapted species) were discriminated on the basis of species properties concerning the xanthophyll cycle functioning and photosynthetic pigments.

Despite the ecophysiological diversity, growth rate and $_{rel}ETR_{max}$ are significantly correlated ($P < 0.025$) in a pooled data set of the three species (Fig. 27). Such evidence suggests how, in these three picoeukaryotes, growth rate is strongly modulated by the electron transport rate driven by the light absorbed within the PSII, and thus how the processes of photoregulation and photoacclimation are efficient in maintaining or enhancing the growth of these species, even under non-optimal light conditions.

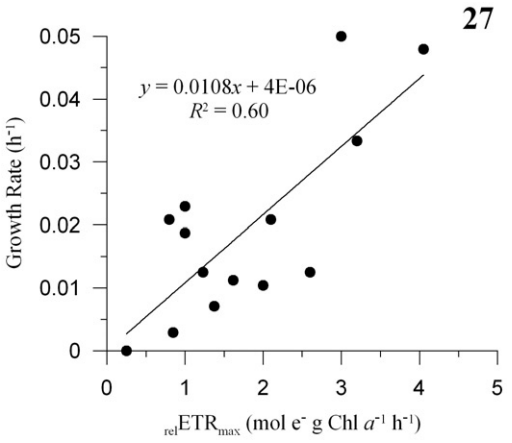

Fig. 27. Relationship between maximal relative electron transport rate, normalized by chlorophyll *a* concentration ($_{rel}ETR_{max}$, expressed in mol e^- g Chl $a^{-1}h^{-1}$), and growth rate (h^{-1}), by pooling the dataset for three picoeukaryotic species: *Minutocellus* sp. RCC703, *Minutocellus* sp. RCC967 and *Phaeomonas* sp. RCC503 (data from Giovagnetti *et al*., 2010).

Acknowledgements

The authors would like to thank F. Tramontano for the help during the experiments and HPLC analysis, as well as V. Saggiomo and F. Margiotta for CHN analysis and for sharing the Phyto-PAM fluorometer. D.A. Campbell and an anonymous reviewer are greatly acknowledged for their comments, which helped to improve the quality of this manuscript. Vasco Giovagnetti's PhD was supported by the Stazione Zoologica A. Dohrn.

References

Armbrust, E.V. (2009). The life of diatoms in the world's oceans. *Nature*, **459**: 185–192.

Brunet, C. & Lavaud, J. (2010). Can the xanthophyll cycle help extract the essence of the microalgal functional response to a variable light environment? *Journal of Plankton Research*, **32**: 1609–1617.

Dimier, C., Corato, F., Saviello, G. & Brunet, C. (2007*a*). Photophysiological properties of the marine picoeukaryote *Picochlorum* RCC237 (Trebouxiophyceae, Chlorophyta). *Journal of Phycology*, **43**: 275–283.

Dimier, C., Corato, F., Tramontano, F. & Brunet, C. (2007*b*). Photoprotection and xanthophyll cycle activity in three diatoms. *Journal of Phycology*, **43**: 937–947.

Dimier, C., Brunet, C., Geider, J.R. & Raven, J.A. (2009*a*). Growth and photo-regulation dynamics of the picoeukaryote *Pelagomonas calceolata* in fluctuating light. *Limnology and Oceanography*, **54**: 823–836.

Dimier, C., Saviello, G., Tramontano, F. & Brunet, C. (2009*b*). Comparative ecophysiology of the xanthophyll cycle in six marine phytoplanktonic species. *Protist*, **160**: 397–411.

Eilers, P.H.C. & Peeters, J.C.H. (1988). A model for the relationship between light intensity and the rate of photosynthesis in phytoplankton. *Ecological Modelling*, **42**: 199–215.

Falkowski, P.G. & Owens, T.G. (1980). Light-shade adaptation: two strategies in marine phytoplankton. *Plant Physiology*, **66**: 592–595.

Falkowski, P.G., Owens, T.G., Ley, A.C. & Mauzerall, D.C. (1981). Effects of growth irradiance levels on the ratio of reaction centers in two species of marine phytoplankton. *Plant Physiology*, **68**: 969–973.

Finkel, Z.V., Beardall, J., Flynn, K.J., Quigg, A., Rees, T.A. & Raven, J.A. (2010). Phytoplankton in a changing world: cell size and elemental stoichiometry. *Journal of Plankton Research*, **32**: 119–137.

Geider, R.J. & Laroche, J. (2002). Redfield revisited: variability of C: N: P in marine microalgae and its biochemical basis. *European Journal of Phycology*, **37**: 1–17.

Giovagnetti, V., Cataldo, M.L., Conversano, F. & Brunet, C. (2010). Functional relation between growth, photosynthetic rate and regulation in the coastal picoeukaryote *Phaeomonas* sp. RCC 503 (Pinguiophyceae, Stramenopiles). *Journal of Plankton Research*, **32**: 1501–1511.

Goliger, A.M. & Retief, J.V. (2002). Identification of zones of strong wind events in South Africa. *Journal of Wind Engineering and Industrial Aerodynamics*, **90**: 1227–1235.

Goss, R. & Jakob, T. (2010). Regulation and function of xanthophyll cycle-dependent photoprotection in algae. *Photosynthesis Research*, doi:10.1007/s11120–010–9536–x.

Grouneva, I., Jakob, T., Wilhelm, C. & Goss, R. (2009). The regulation of xanthophyll cycle activity and of non-photochemical fluorescence quenching by two alternative electron flows in the diatoms *Phaeodactylum tricornutum* and *Cyclotella meneghiniana*. *Biochimica et Biophysica Acta*, **1787**: 929–938.

Guillard, R.R. & Ryther, J.H. (1962). Studies of marine planktonic diatoms. I. *Cyclotella nana* Hustedt and *Detonula confervacea* (Cleve) Gran. *Canadian Journal of Microbiology*, **8**: 229–238.

Havaux, M. & Niyogi, K.K. (1999). The violaxanthin cycle protects plants from photooxidative damage by more than one mechanism. *Proceedings of the National Academy of Sciences USA*, **96**: 8762–8767.

Hedges, J.I. & Stern, J.H. (1984). Carbon and nitrogen determination of carbonate-containing solids. *Limnology and Oceanography*, **29**: 657–663.

Key, T., Mccarthy, A., Campbell, D.A., Six, C., Roy, S. & Finkel, Z.V. (2009). Cell size trade-offs govern light exploitation strategies in phytoplankton. *Environmental Microbiology*, doi:10.1111/j.1462–2920.2009.02046.x.

Kooistra, W.H.C.F., Gersonde, R., Medlin, L.K. & Mann, D.G. (2007). The origin and evolution of the diatoms: their adaptation to a planktonic existence. In *Evolution of Primary Producers in the Sea* (Falkowski, P.G. & Knoll, A.H., editors), 207–249. Elsevier Academic Press, Burlington, MA.

Lavaud, J., Rousseau, B., van Gorkom, H.J. & Etienne, A.-L. (2002*a*). Influence of the diadinoxanthin pool size on photoprotection in the marine planktonic diatom *Phaeodactylum tricornutum*. *Plant Physiology*, **129**: 1398–1406.

Lavaud, J., Rousseau, B. & Etienne, A.-L. (2002*b*). In diatoms, a transthylakoidal proton gradient alone is not sufficient for non-photochemical fluorescence quenching. *FEBS Letters*, **523**: 163–166.

Lavaud, J., Rousseau, B. & Etienne, A.-L. (2004). General features of photoprotection by energy dissipation in planktonic diatoms (Bacillariophyceae). *Journal of Phycology*, **40**: 130–137.

Lavaud, J., Strzepek, R.F. & Kroth, P.G. (2007). Photoprotection capacity differs among diatoms: possible consequences on the spatial distribution of diatoms related to fluctuations in the underwater light climate. *Limnology and Oceanography*, **52**: 1188–1194.

Le Gall, F., Rigaut-Jalabert, F., Marie, D., Garczarek, L., Viprey, M., Godet, A. & Vaulot, D. (2008). Picoplankton diversity in the South-East Pacific Ocean from cultures. *Biogeosciences*, **5**: 203–214.

Lepetit, B., Goss, R., Jakob, T. & Wilhelm, C. (2012). Molecular dynamics of the diatom thylakoid membrane under different light conditions. *Photosynthesis Research*, **111**: 245–257.

Li, Z., Wakao, S., Fischer, B.B. & Niyogi, K.K. (2009). Sensing and responding to excess light. *Annual Review of Plant Biology*, **60**: 239–260.

Litchman, E. & Klausmeier, C.A. (2008). Trait-based community ecology of phytoplankton. *Annual Review of Ecology Evolution and Systematics*, **39**: 615–639.

Lohr, M. & Wilhelm, C. (1999). Algae displaying the diadinoxanthin cycle also possess the violaxanthin cycle. *Proceedings of the National Academy of Sciences USA*, **96**: 8784–8789.

Lohr, M. & Wilhelm, C. (2001). Xanthophyll synthesis in diatoms: quantification of putative intermediates and comparison of pigment conversion kinetics with rate constants derived from a model. *Planta*, **212**: 382–391.

Lynn, S.G., Kilham, S.S., Kreeger, D.A. & Interlandi, S.J. (2000). Effect of nutrient availability on the biochemical and elemental stoichiometry in the freshwater diatom *Stephanodiscus minutulus* (Bacillariophyceae). *Journal of Phycology*, **36**: 510–522.

Macintyre, H.L., Kana, T.M. & Geider, R.J. (2000). The effect of water motion on short-term rates of photosynthesis by marine phytoplankton. *Trends in Plant Science*, **5**: 12–17.

Not, F., Massana, R., Latasa, M., Marie, D., Colson, C., Eikrem, W., Pedrós-Alió, C., Vaulot, D. & Simon, N. (2005). Late summer community composition and abundance of photosynthetic picoeukaryotes in Norwegian and Barents Sea. *Limnology and Oceanography*, **50**: 1677–1686.

Raven, J.A. (1998). The twelfth Tansley lecture. Small is beautiful: the picophytoplankton. *Functional Ecology*, **12**: 503–513.

Raven, J.A. & Geider, J.R. (2003). Adaptation, acclimation and regulation in algal photosynthesis. In *Photosynthesis in Algae, Advances in photosynthesis and respiration Vol. 14* (Larkum, W.D., Douglas, S.E. & Raven, J.A., editors), 385–412. Kluwer Academic Publishers, Dordrecht, the Netherlands.

Raven, J.A., Finkel, Z.V. & Irwin, A.J. (2005). Picophytoplankton: bottom-up and top-down controls on ecology and evolution. *Vie Milieu*, **55**: 209–215.

Six, C., Finkel, Z.V., Rodriguez, F., Marie, D., Partensky, F. & Campbell, D.A. (2008). Contrasting photoacclimation costs in ecotypes of the marine eukaryote picoplankter *Ostreococcus*. *Limnology and Oceanography*, **53**: 255–265.

Six, C., Sherrard, R., Lionard, M., Roy, S. & Campbell, D.A. (2009). Photosystem II and pigment dynamics among ecotypes of the Green Alga *Ostreococcus*. *Plant Physiology*, **151**: 379–390.

Smetacek, V. (1999). Diatoms and the ocean carbon cycle. *Protist*, **150**: 25–32.

Stransky, H. & Hager, A. (1970). Das Carotinoidmuster und die verbreitung des lichtinduzierten Xanthophyllcyclus in verschiedenen algenklassen. *Archives of Microbiology*, **71**: 164–190.

Strzepek, R.F. & Harrison, P.J. (2004). Photosynthetic architecture differs in coastal and oceanic diatoms. *Nature*, **431**: 689–692.

Wagner, H., Jakob, T. & Wilhelm, C. (2006). Balancing the energy flow from captured light to biomass under fluctuating light conditions. *New Phytologist*, **169**: 95–108.

Wilhelm, C., Büchel, C., Fisahn, J., Goss, R., Jakob, T., Laroche, J., Lavaud, J., Lohr, M., Riebesell, U., Stehfest, K., Valentin, K. & Kroth, P.G. (2006). The regulation of carbon and

nutrient assimilation in diatoms is significantly different from green algae. *Protist*, **157**: 91–124.

Worden, A.Z. & Not, F. (2008). Ecology and diversity of picoeukaryotes. In *Microbial Ecology of the Oceans, Second Edition* (Kirchman, D.L., editor), 159–205. John Wiley & Sons, New York.

Vaulot, D., Le Gall, F., Marie, D., Guillou, L. & Partensky, F. (2004). The Roscoff Culture Collection (RCC): a collection dedicated to marine picoplankton. *Nova Hedwigia*, **79**: 49–70.

Vaulot, D., Eikrem, W., Viprey, M. & Moreau, H. (2008). The diversity of small eukaryotic phytoplankton ($\leq$3 μm) in marine ecosystems. *FEMS Microbiology Reviews*, **32**: 795–820.